Cold Regions Science and Technology 190 (2021) 103344

Contents lists available at ScienceDirect

Cold Regions Science and Technology

journal homepage: www.elsevier.com/locate/coldregions

Intercomparison of UAV platforms for mapping snow depth distribution in complex alpine terrain

Jesús Revuelto [a,*], Esteban Alonso-Gonzalez [a], Ixeia Vidaller-Gayan [a], Emilien Lacroix [b], Eñaut Izagirre [c], Guillermo Rodríguez-López [d], Juan Ignacio López-Moreno [a]

[a] Instituto Pirenaico de Ecología, Consejo Superior de Investigaciones Científicas (IPE-CSIC), Zaragoza, Spain
[b] Université Grenoble Alpes, Grenoble, France
[c] Department of Geology, University of the Basque Country UPV/EHU, 48940 Leioa, Spain
[d] Departamento de Geografía y Ordenación del Territorio, Universidad de Zaragoza, Spain

ARTICLE INFO

Keywords:
Unmanned aerial vehicles
Intercomparison
Multi-rotors
Fixed wings
Snow depth mapping
Mountain areas

ABSTRACT

Unmanned Aerial Vehicles (UAVs) offer great flexibility in acquiring images in inaccessible study areas, which are then processed with stereo-matching techniques through Structure-from-Motion (SfM) algorithms. This procedure allows generating high spatial resolution 3D point clouds. The high accuracy of these 3D models allows the production of detailed snow depth distribution maps through the comparison of point clouds from different dates. In this way, UAVs allow monitoring of remote areas that were not achievable previously. The large number of works evaluating this novel technique has not, to date, conducted a systematic evaluation of concurrent snowpack observations with different UAV devices. Taking into account this, and also bearing in mind that potential users of this technique may be interested in exploiting ready-to-use commercial devices, we conducted an evaluation of the snow depth distribution maps with different commercial UAVs. During the 2018–19 snow season, two multi-rotors (*Parrot Anafi* and *DJI Mavic Pro2*) and one fixed-wing device (*SenseFly eBee plus*) were used on three different dates over a small test area (5 ha) within Izas Experimental Catchment in the Central Pyrenees. Simultaneously, snowpack distribution was retrieved with a Terrestrial Laser Scanner (TLS, *RIEGL LPM-321*) and was considered as ground truth. Three different georeferencing methods (Ground Control Points, ICP algorithm over snow-free areas and RTK-GPS positioning) were tested, showing equivalent performances under optimum illumination conditions. Additionally, for the three acquisition dates, both multi-rotors were flown at two distinct altitudes (50 and 75 m) to evaluate impact on the obtained snow depth maps. The evaluation with the TLS showed an equivalent performance of the two multi-rotors, with mean RMSE below 0.23 m and maximum volume deviations of less than 5%. Flying altitudes did not show significant differences in the obtained maps. These results were obtained under contrasted snow surface characteristics. This study reveals that under good illumination conditions and in relatively small areas, affordable commercial UAVs provide reliable estimations of snow distribution compared to more sophisticated and expensive close-range remote sensing techniques. Results obtained under overcast skies were poor, demonstrating that UAV observations require clear-sky conditions and acquisitions around noon to guarantee a homogenous illumination of the study area.

1. Introduction

Having detailed information of snowpack distribution and its temporal evolution in remote mountain areas is required for understanding many mountain processes, such as glacier surface mass balance (Hock, 2005; Hock et al., 2017; Réveillet et al., 2017) or hydrological response of mountain rivers (Fayad et al., 2017; Pomeroy et al., 2004). This has motivated many scientific works aiming to obtain reliable snowpack observations in heterogeneous mountain areas. Distinct remote sensing techniques have been used to retrieve snowpack distribution in remote areas, such as terrestrial and airborne laser scanning (Deems et al., 2013; Grünewald et al., 2010; Prokop, 2008), satellite sensors (Frei et al., 2012; Parajka and Blöschl, 2008) or time-lapse photography (Parajka et al., 2012; Revuelto et al., 2016a). In the last five years, Structure-for-

* Corresponding author.
E-mail address: jrevuelto@ipe.csic.es (J. Revuelto).

https://doi.org/10.1016/j.coldregions.2021.103344
Received 26 November 2020; Received in revised form 27 June 2021; Accepted 28 June 2021
Available online 30 June 2021

Motion (SfM) photogrammetry applied to images acquired by Unmanned Aerial Vehicles (UAVs) has been frequently utilized by the snow science community (Adams et al., 2018; Eberhard et al., 2021; Gaffey and Bhardwaj, 2020; Harder et al., 2016). The method for obtaining snow depth distribution maps is simply subtracting two 3D point clouds generated with stereo matching techniques (through SfM algorithms) from UAV-acquired images on two distinct dates, one corresponding to a snow-free period and the other to snow-covered terrain. Recent technical developments in the field of electronics and battery endurance (Chang and Yu, 2015; Traub, 2011) have permitted an important reduction of the battery/UAV device weight ratio, enabling longer flights and thus covering extended areas, not achievable previously. The latest improvements of SfM algorithms (Snavely et al., 2006; Westoby et al., 2012) have shown compelling results under challenging terrain textures such as snow, boosting its application in many study areas worldwide (Cimoli et al., 2017; De Michele et al., 2016; Fernandes et al., 2018; Goetz and Brenning, 2019; Harder et al., 2020; Nolan et al., 2015).

The application of UAVs for observing the snowpack in remote mountain areas has many benefits when compared to preceding methods. For instance, UAVs allow data collection over extended areas, decreasing human exposure to mountain hazards such as snow avalanches and rockfalls. Moreover, the bird's eye point view of UAVs enable the acquisition of observations over the entire target area, something that is not achievable with terrestrial close-range remote sensing devices such as multi-station or Terrestrial Laser Scanners (TLS), due to topographical shadowing effects (Avanzi et al., 2018; Revuelto et al., 2014a). UAVs also have relatively fast acquisition times compared to manual acquisition (López-Moreno et al., 2011). Currently, there are a wide variety of commercial UAVs and SfM software with user-friendly interface, allowing application of this technique in a broad community of cryosphere scientists (Gaffey and Bhardwaj, 2020). However, the generation of detailed snow distribution cartographies with UAVs is still limited by various shortcomings. For instance, SfM algorithms may have important deviations on 3D reconstruction of homogenous surfaces when illumination is not regular (i.e. shadows cast from the terrain) (Boesch et al., 2016; Cimoli et al., 2017; Gindraux et al., 2017). Another relevant point is the occurrence of patchy snow distribution; shallow snowpack measurements are less likely to be appropriately retrieved with this methodology (De Michele et al., 2016; Harder et al., 2016).

Currently, processing UAV-acquired images with SfM software is affordable and does not require a particularly high degree of skill in geomatics. It is thus accessible for researchers from different disciplines. Nonetheless, generalization in the use of this technique requires precise identification of errors the snow science community could expect from this novel technique. Additionally, the fast changing meteorological conditions that characterize mountain areas, show the need for a comprehensive evaluation of UAV reliability when mapping snow distribution under different weather and snowpack conditions (Vander Jagt et al., 2013). There is currently a wide variety of UAV platforms available on the market, with strong differences among them in characteristics such as battery endurance, flight type, geotagging options and price. The UAV platform characteristics and the sensor mounted on it, can also influence the reliability of the final UAV observations(Adams et al., 2018; De Michele et al., 2016). New users may face a dilemma deciding which type of UAV may fulfil their needs while achieving a good balance between the quality of the obtained snow maps against the complexity of the experimental design and the expected cost. This study presents an evaluation of the snow depth maps generated with two relatively low-cost multi-rotors UAVs and a more sophisticated fixed wing UAV (which must be flown at higher elevations for safety reasons) having Real Time Kinematic (RTK) processing of the GPS signal (centrimetric positioning accuracy); with snow maps obtained from a TLS, the latter being considered as ground truth with estimated errors for measuring snow depths under 10 cm (Prokop, 2008; Revuelto et al., 2014a). The effects of light conditions and flying altitude on the quality and accuracy of snow depth maps are analysed and discussed.

2. Study area and period

This study was conducted in the Izas Experimental Catchment, a high mountain catchment with a long record of hydrological and meteorological observations (Revuelto et al., 2017). This experimental site is located in the Central Spanish Pyrenees (42°44′ N, 0°25′ W; Fig. 1), close to the main divide of the mountain range. Its elevation ranges from 2000 to 2300 m above sea level (a.s.l.) and has a main slope of 16° with a highly heterogeneous topography. Except for some rocky outcrops, the catchment is covered by alpine grassland. This study area has a long record of snow-related studies (Anderton et al., 2002, 2004; López-Moreno et al., 2011, 2012, 2015; Revuelto et al., 2014b, 2016a, 2016b, 2020) and thus it has an experimental setup allowing precise observation of the snowpack. Its elevation guarantees a remarkable presence of snow from November to the end of May (López-Moreno et al., 2010). Despite the total surface of the catchment having more than 50 ha, this study defined a smaller test area of about 5 ha in the centre of the study site, where gullies and ridges alternate with a flat area (Fig. 1).

This study site is equipped with an automatic weather station (Revuelto et al., 2017). Additionally, in the eastern corner of the study site, a webcam acquires three images per day of nearly 30% of the catchment (Fig. 1), from which the daily snow covered area extent is retrieved (Corripio, 2004; Revuelto et al., 2016a). The information obtained from these fully autonomous sensors allows detailed monitoring of snow cover evolution during the study period, which spans from 21 February 2019 to 30 May 2019. Fig. 2 shows the evolution of the snow covered area (SCA) and both snow depth and daily precipitation registered at the automatic weather station. The 2018–19 snow season was characterized by below-average snow accumulation, with several accumulation and melt periods, which is a significant characteristic of the snowpack dynamics in the Pyrenees (López-Moreno, 2005).

3. Methodology

For three acquisition dates, 21 February 2019, 9 May 2019 and 30 May 2019, the test area was observed with four different devices which exploited two distinct remote sensing techniques for generating 3D point clouds of the target surface. Three out of these four devices are UAVs that acquire images of a target area with a remarkable overlap among them that subsequently allows the generation of a 3D point cloud with SfM algorithms. The fourth device is a TLS using LiDAR (Light Detecting and Ranging) technology, which also produces a 3D point cloud of the target area through the acquisition of distances from the device to hundreds of thousands of points of the surveyed surface.

3.1. UAV platforms and flight configurations

The three UAV platforms (Fig. 3) evaluated were two multi-rotors (the *Parrot Anafi*, and *DJI Mavic Pro 2* quad-copters) and one fixed wing with RTK-GPS positioning (*SenseFly eBee-Plus*). The RTK-GPS positioning of the fixed wing UAV is achieved via a virtual RTK base station, calculated through a real time triangulation of the closest stations from the local geodesic network accessed via internet. The virtual base station is computed in *emotion 3* (the *eBee-Plus* controller software) for the location where the UAV is turned-on. The RTK-GPS correction is obtained through the radio modem communication with the UAV through this software. The three UAVs are commercial devices that allow a relatively simple set up of their flight missions with self-operating image acquisition once the devices have been launched. The camera sensors of the three UAVs have similar characteristics (Table 1) generating JPG images. This equivalence in camera resolution and sensor technology is relevant, since it allows assessing differences related to the overall UAV characteristics and decreases potential discrepancies coming from remarkable differences of the sensor.

For each acquisition date, the three UAVs were flown with a maximum temporal difference of 40 min to avoid major differences in

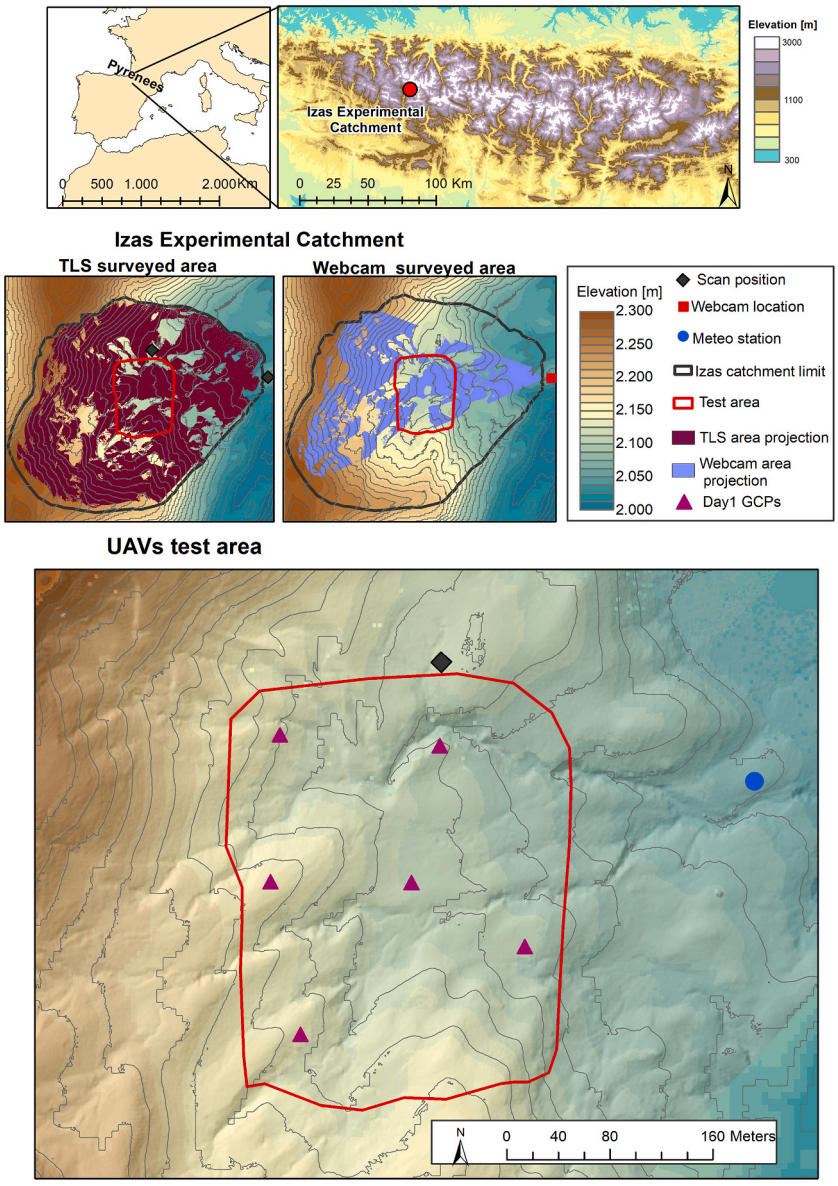

Fig. 1. Study area location and topography. Top maps show the location of the Izas Experimental Catchment in the Pyrenees. Middle maps depict the extent of information retrieved with the experimental setup of the two long-lasting remote sensing techniques observing snow distribution in this site, time-lapse webcam monitoring of the snow cover and snow depth acquisitions with a TLS. Bottom map display a zoom of the test area, showing the heterogeneity of the topography.

the test area, including meteorological conditions (wind or illumination changes due to changes in cloud presence) and potential changes in snowpack (remarkable height or surface changes). *Anafi* and *Mavic* flights were configured with the same software *Pix4Dcapture* and observations were repeated at two flight altitudes, 50 m and 75 m above take off position. For both altitudes, the longitudinal and the lateral overlap of the images was respectively 85% and 70%, which is appropriate for observing snow covered areas (Harder et al., 2016; Vander Jagt et al., 2015). These overlaps were also maintained in the flight configuration of the *eBee* flights, which were configured in *emotion3* software (Revuelto et al., 2021). In contrast, the fixed-wing UAV flight altitude was set to 120 m. This altitude guarantee a good compromise between a safe flight (note that fixed wing UAVs have high operation speeds when compared with multi-rotors and this is an important constrain in mountain areas) and the ground sampling distance (distance between two consecutive camera pixel centres measured on the ground), which for 120 m flight altitude, is 2.8 cm /pixel.

3.2. Generation of georeferenced 3D point clouds

The images acquired in the different flights with the three UAV platforms were processed with the same SfM software, *Pix4Dmapper* (version 4.4.12). Specially designed for processing drone images, this software provides a complete report on the quality and accuracy of the 3D information generated. The SfM algorithms of *Pix4Dmapper* have distinct options for generating full or moderate resolution point clouds; however, the impact for mapping snow depth distribution in mountain areas is known to be negligible (Revuelto et al., 2021). Therefore, the faster processing options were used here to generate the 3D surface of each flight.

All point clouds were generated in the European Terrestrial Reference System 1989 (ETRS 89), in the UTM 30 N projection. The *eBee-Plus* images were georeferenced with accuracy below 2 cm during the flights exploiting the GPS-RTK positioning of this UAV (Forlani et al., 2018). In contrast *Anafi,* or *Mavic2Pro* UAVs does not allow such an accurate geotagging of the images, and their coordinates have the standard error

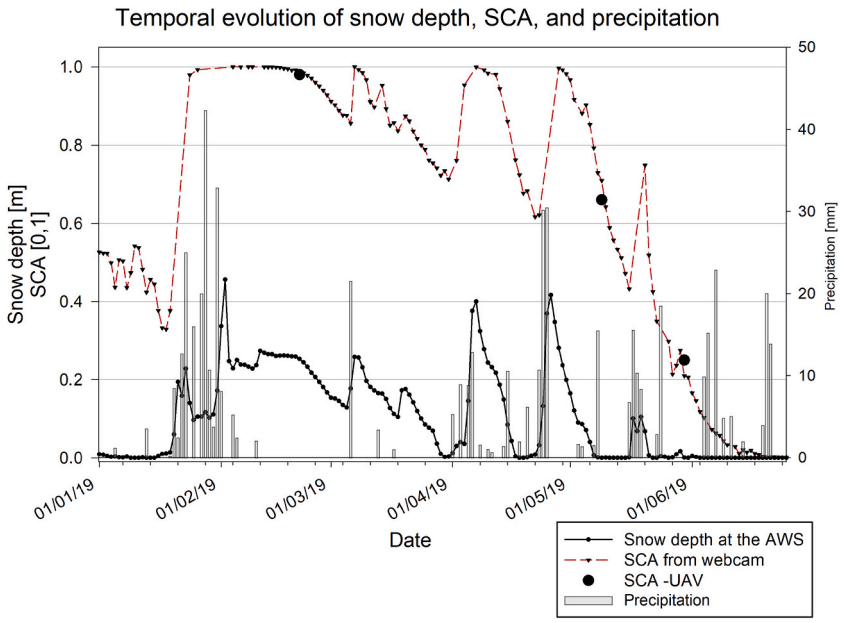

Fig. 2. Daily evolution of the snow depth, snow covered area retrieved with the experimental setup installed in the Izas Experimental Catchment. It also includes the snow covered area observed with the fixed-wing UAV for the three experimental campaigns.

Fig. 3. Picture of the three UAV platforms tested in this work. Parrot Anafi on the left, Sensefly eBee Plus in the centre and DJI Mavic Pro 2 on the right.

Table 1
Main technical specifications, from the official datasheets, of the three UAVs.

UAV	Weight	Flight tech.	Dimensions [cm]	Autonomy	Max Wind speed res.	GPS with RTK	Camera Resolution	Lenses
Anafi	320 g	Quad-copter	17,5 × 23,8 × 6,3	25 min.	50 km/h	No	21 Mp (1/2,4" CMOS sensor)	f/2.4 (35 mm equivalent: 23–69 mm)
Mavic	907 g	Quad-copter	32,2 × 24 × 8,4	31 min	38 km/h	No	20Mp 1" CMOS sensor 2472 × 3648	f/2.8 - f/11 (35 mm equivalent: 28 mm)
eBee	1100 g	Fixed-wing	110 cm (wing spam)	59 min	46 km/h	Yes	20Mp 1" CMOS sensor 3648 × 5472	f/2.8 - f/11, (35 mm equivalent: 29 mm)

of regular GPS. Thus, images obtained with these devices had position accuracy of 5 m. For a precise and accurate representation of the snow depth distribution, alternative methods (to RTK positioning) are needed to establish absolute position of the multi-rotors generated point clouds.

To date, most UAV studies retrieving snow depth distribution have used indirect positioning of the 3D point clouds through Ground Control Points (GCP), with an accurate positioning obtained with differential GPS technique (Adams et al., 2018; Avanzi et al., 2018; De Michele et al., 2016). Point clouds of the two multi-rotor devices had to be georeferenced with GCPs, homogenously distributed in the study area, placing on them recognizable targets from bird's eye point of view (Agüera-Vega et al., 2017). On 21 February 2019, six GCPs were established within the

test area. On each GCP a 0.5 × 0.5 m squared panel was placed, and their central positions were obtained with the TLS. Using the target scanning mode of the TLS, the coordinates of the GCPs were obtained, with a standard deviation of 0.03 m. These coordinates were introduced in *Pix4Dmapper* GCP manager tool, which allows identifying target locations on a preliminary point cloud and, subsequently, generates a pointcloud with centimetric positioning accuracy.

For the other two acquisition dates, a novel procedure was tested which co-registered point clouds to the snow-free model. We took advantage of the existence of easily identifiable snow-free areas to apply co-registration. The snow-free areas from the point clouds generated on 9 May and 30 May were then aligned to the *eBee* snow-free point cloud, using the Iterative Closest Point (ICP) algorithm (Besl and McKay, 1992; Rajendra et al., 2014). Initially, the point clouds were generated in *Pix4Dmapper* with the same accuracy as the UAV images geotagging (5 m). Subsequently, the snow-free areas of the point clouds were selected in *CloudCompare*. The overlap percentage between both point clouds in the ICP tool was the percentage of the snow-free area derived from RGB data (with a threshold value in the blue channel to classify snow-free and snow-covered areas (Revuelto et al., 2016a)). This guarantees an alignment of the rotary devices point clouds which included only areas corresponding to the same surface.

The ICP tool of this later software calculated the rotation and translation matrix to align the UAV point cloud to the snow-free point cloud of the test area Since ICP is an iterative process, a minimum reduction on the Root Mean Squared Error (RMSE) of 1.0e-5 between consecutive iterations was set up in a three-step process; a first random selection of 5000, a second of 50,000 and a third of 500,000 points. Finally, the rotation and translation matrix obtained after these three steps was applied to the complete point cloud, comprising snow-covered and snow -free areas.

Table 2 gives details on the final RMSE obtained for the three acquisition dates. It should be noted that for either the GCP registration of *Pix4Dmapper* or for the ICP alignment of *CloudCompare*, the coordinates used as reference are affected by the same standard deviation (0.03 m) associated to the global coordinate system transformation of TLS acquisitions at Izas Experimental Catchment (Revuelto et al., 2014a).

3.3. Generation of snow depth distribution maps

Snow depth distribution maps are obtained rasterizing the difference between two 3D point clouds corresponding to two distinct dates, one obtained from UAV images retrieved under snow-free conditions and the other with UAV images captured on snow-covered conditions. The snow-free flight was conducted on 25 July 2019 with the fixed wing UAV. The snow-on and snow-free point cloud distances were obtained with the *Multiscale Model to Model Cloud Comparison* tool (James et al., 2017; Lague et al., 2013) of *Cloud Compare*. Finally, the snow depth maps were rasterized with a 1 × 1 m grid cell size known to provide reliable spatial patterns in small to medium sized domains (Grünewald and Lehning, 2015; Schön et al., 2018). Following a similar method, details on how the TLS snow depth maps were obtained, combining the information acquired from two scan positions(Fig. 1), are described in (Revuelto et al., 2014a).

3.4. Evaluation of UAV capabilities for mapping snow depth distribution

Snow depth maps generated for the three acquisition dates with the two multi-rotors UAVs at two flight altitudes (50 and 75 m) and the *eBee* acquisitions were compared, using TLS snow depth maps. The accuracy of UAV snow depth observations was assessed through the *Mean Absolute Error* (MAE) and the *Root Mean Squared Error* (RMSE). As a measure of precision we computed the *Normalized Median Absolute Deviation* (NMAD; Höhle and Höhle, 2009). Other metrics were also computed, such as the total snow volume difference between the snow depth maps (as a % of the reference) and both the mean snow depth and the standard deviations of the snow-covered pixels. This approach allows evaluation of the reliability of the final UAV product, from the end user point of view, providing potential deviations that may be expected under different snow and meteorological conditions.

4. Results

Fig. 4 shows that, with the four remote sensing devices compared here, it is feasible to generate reliable snow depth distribution maps when a well-established acquisition and post-processing protocol is applied. Despite some small differences observed among the six snow depth maps, the main patterns of snow distribution are well reproduced independent of UAV and flight altitude. However, in areas with a shallow snowpack, some deviations among the maps are observed. In these plots, one of the major drawbacks of TLS acquisitions is also identified - no data zones (black areas of bottom left map in Fig. 4) due to topographic shadowing from the device point of view, reducing the extent of the surveyed area (Table 3). Such a limitation is overcome in the UAV acquisitions because their bird's eye point of view allows retrieval of information from the entire test area, under good illumination conditions such as those of 21 February (Fig. 4), generating snow depth maps with a negligible incidence of no data areas.

The snow-covered area percentage changed during the study period (Fig. 2 and Table 3) as a result of the inherent evolution of the snowpack. Similarly, the percentage of the test area from which each device was able to retrieve observations was not the same for the three acquisition dates (Table 3). For two out of the three UAVs, the extension of the point cloud generated by the SfM algorithms was highly affected by illumination issues (Fig. 5), with a decrease on the surveyed surface ranging from 11% to 21% on 9 May 2019.

On 9 May 2019, a thick cloud cover impeded direct sunlight over the test area during the UAV acquisition and thus; flights, were conducted with an overcast sky. This illumination issue reduced the extent of the generated point clouds, which led to a decrease in the extent of snow depth maps. Similarly, point cloud densities were markedly reduced for flights obtained this later date (Table 4). These results also show the decrease in point cloud densities when flying at higher altitudes.

The impact of direct solar radiation or lack of (Fig. 5), on SfM algorithms to appropriately recognize snow surfaces can be noticed in light of the images of Fig. 6. Under clear sky conditions, UAV cameras are able to retrieve snow textures detailed enough allowing an efficient computation of stereo matching algorithms and accomplishing a suitable densification of the point cloud (see left side representations of the 3D point clouds and the orthophotos under different sky conditions in Fig. 6).

Mean snow depths and standard deviations obtained in the common area of the TLS and the UAVs (Fig. 7) show a good agreement for the two

Table 2
Root mean squared error of the point clouds georeferencing for the three acquisition dates and the different UAV flights.

	Date	Method	Anafi_50m	Anafi_75m	Mavic_50m	Mavic_75m
Day 1	21/02/2019	GCP (6)	0.012 m	0.015 m	0.005 m	0.006 m
Day 2	09/05/2019	ICP	0.105 m	0.124 m	0.246 m	0.186 m
Day 3	30/05/2019	ICP	0.07 m	0.081 m	0.084 m	0.074 m

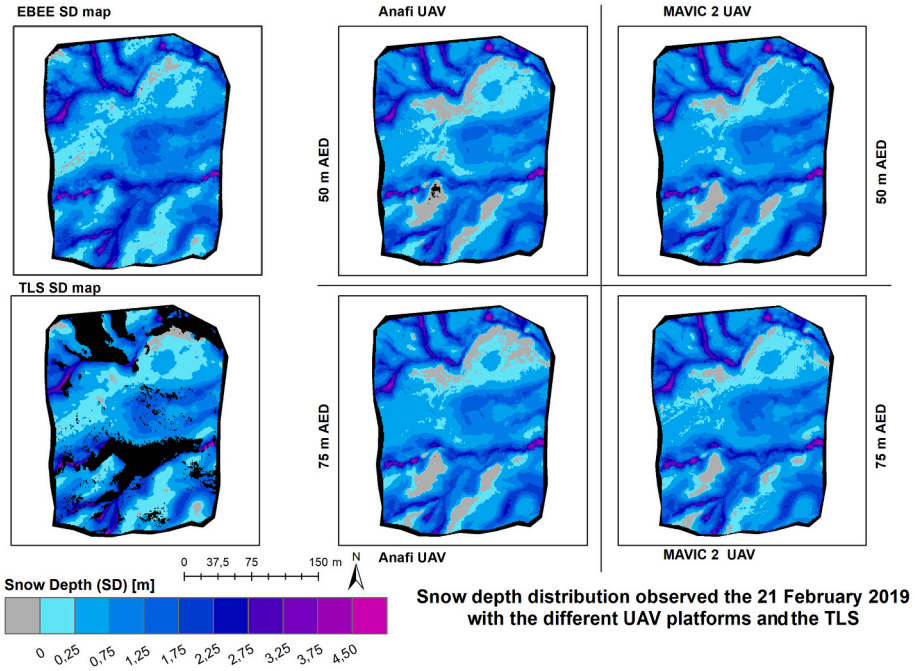

Fig. 4. Snow depth map obtained on 21 February 2019 with the four remote sensing devices. Centre and right snow maps depict snow distribution for the two flight altitudes tested with the two rotary devices.

Table 3
Snow-covered area and percentage of the test area with valid information for the three acquisition dates and the four remote sensing devices exploited.

	Snow Covered Area percentage				Percentage of the test area with valid information			
Date	TLS	eBbee	Mavic	Anafi	TLS	eBbee	Mavic	Anafi
21 Februray2019	99,5	94,6	94,3	95	76	98	97	99
9 May 2019	91,2	70	74,8	78,6	77	79	99	89
30 May2019	23	33,9	36,9	37,1	77	99	99,8	100

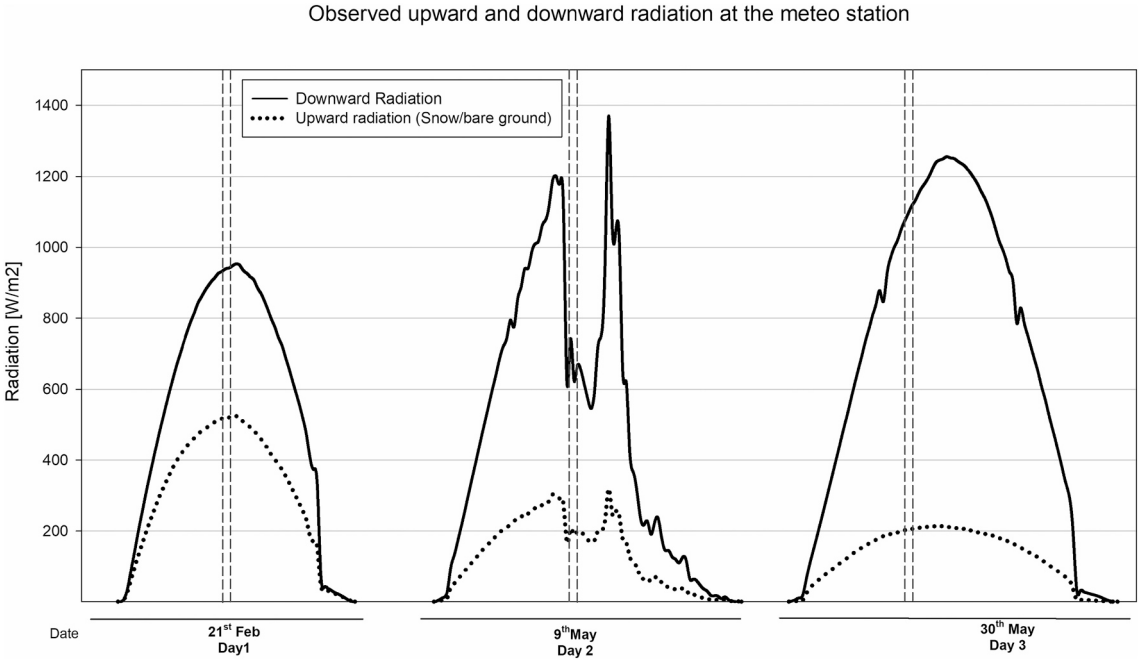

Fig. 5. Upward and downward radiation observed at the automatic weather stations of Izas Experimental Catchment for the three acquisition dates. Vertical dashed lines denote the time interval of UAV acquisitions.

Table 4
Point clouds densities obtained with the images from the different UAV flights in the three acquisitions dates.

Date	Flight altitude	eBee (fly altitude 120 m) [Pts/m^3]	Mavic [Pts/m^3]	Anafi [Pts/m^3]
21 February 2019	50 m	15.3	65.3	72.2
	75 m		33.7	40.1
9 May 2019	50 m	3.6	20.2	14.6
	75 m		7.4	4.8
30 May 2019	50 m	43.1	80.5	78.3
	75 m		50.2	45.1

acquisition dates under good illumination conditions (the 21 February2019 and the 31 May 2019). Mean values for the first and third acquisition dates had the deepest and shallowest snow depth, respectively and a better agreement with the TLS. Both days had good lighting conditions. Mean values obtained for the second acquisition date, with an overcast sky, showed bad agreement with the TLS. This shows decreased reliability of snow depth observations under bad illumination conditions. Flight altitude had very little impact on estimated accuracy for *Anafi* and *Mavic;* the accuracy was slightly better when flying at 75 m.

Error estimations obtained with the TLS evaluation (Fig. 8) show very high deviations for the second acquisition date. The first and third acquisition dates, with a thick snowpack and the test area mostly snow covered (Table 3), or with a shallow snowpack and snow cover below 40% have RMSE lower than 0.3 m and MAE smaller than 0.25 m. Under optimum lighting conditions, the average RMSE is 0.25 m for the *Anafi*, 0.21 m for the *Mavic,* and 0.17 m for the *eBee*. Similarly, total snow volume differences are lower than 10% for the two dates with direct solar radiation. Also, the NMAD has low values for the two acquisition dates with good lighting conditions (21 February 2019 and 31 May 2019), with average NMAD of 0.16 m for the *Anafi* and 0.14 m for the *Mavic*, whereas the 9 May 2019 under bad lighting conditions this error estimate increased noticeably. Mean absolute volume difference comprising first and third day acquisitions for the *Anafi* snow depth maps have a deviation of 3% from the TLS observations, 2.5% in the *Mavic* observations and less than 1.5% for the *eBee* snow depth maps. Conversely, volume differences are higher than 25% under bad light conditions for the two multi-rotors and near 20% for the fixed wing device.

The UAV snow depth maps have a larger area than those of the TLS (Table 3), having information in maximum accumulation areas not retrieved with the TLS (Fig. 4). In this regard, and considering ground truth, the *eBee* observations provided better UAV snow depth observations under good illumination conditions, when compared to the TLS observations. Error estimations were obtained for the *Mavic* and the *Anafi* observations on the first and third acquisition dates (supplementary material). These two dates yield average RMSE of 0.2 m and 0.18 m respectively for the *Anafi* and *Mavic* snowpack observations. Volume differences were, on average, 5% for the *Anafi* and 4.3% for the *Mavic* observations. These results show an equivalent performance of the UAV platforms tested here for dates with direct solar radiation over the entire study area.

In general, higher flight altitudes (75 m) yielded slightly more reliable snow depth distribution maps with both multi-rotors. The large deviations obtained for the second acquisition date, under an overcast sky, demonstrate the major impact of lighting conditions on UAV snowpack observations, compared to flight altitude.

5. Discussion

UAVs have shown compelling results for the observation of snowpack distribution in small- to medium-sized domains (Avanzi et al., 2018; Goetz and Brenning, 2019; Harder et al., 2016). However, to date there has not been a simultaneous intercomparison of different UAV models for observing snow surfaces performed. In this study, two widely used and affordable multi-rotors (*Parrot Anafi* and *DJI Mavic Pro 2*) were tested, along with a more sophisticated commercial, ready-to-use, fixed-wing UAV (*SenseFly eBee- Plus*). Snow maps were compared to data collected with a TLS, which is considered as ground truth (snow depth estimated error below 10 cm, Revuelto et al., 2014a). It is relevant to highlight here that the snow depth maps derived from the three UAVs, exploited the same snow-free point cloud (a summer *eBee plus* acquisition) to compute the snow depth distribution. This way, the snow depth maps evaluated are not fully independent, since snow depth errors will depend on both error in the snow-free and snow-covered surfaces. Hereby, the evaluations shown in this work are indirectly assessing differences in the snow surface error through errors in the snow depth estimations. In turn, the indirect assessment of the snow surface errors of

Fig. 6. Middle panel images: eBee Images of the same location corresponding to the first and second acquisition dates. Left side panel images: Point clouds generated with the images acquired with the Anafi UAV. These panels also depict two images of the study area acquired during the UAV flights, showing the sky conditions. Right panels show the orthophotos generated for each Anafi UAV flight.

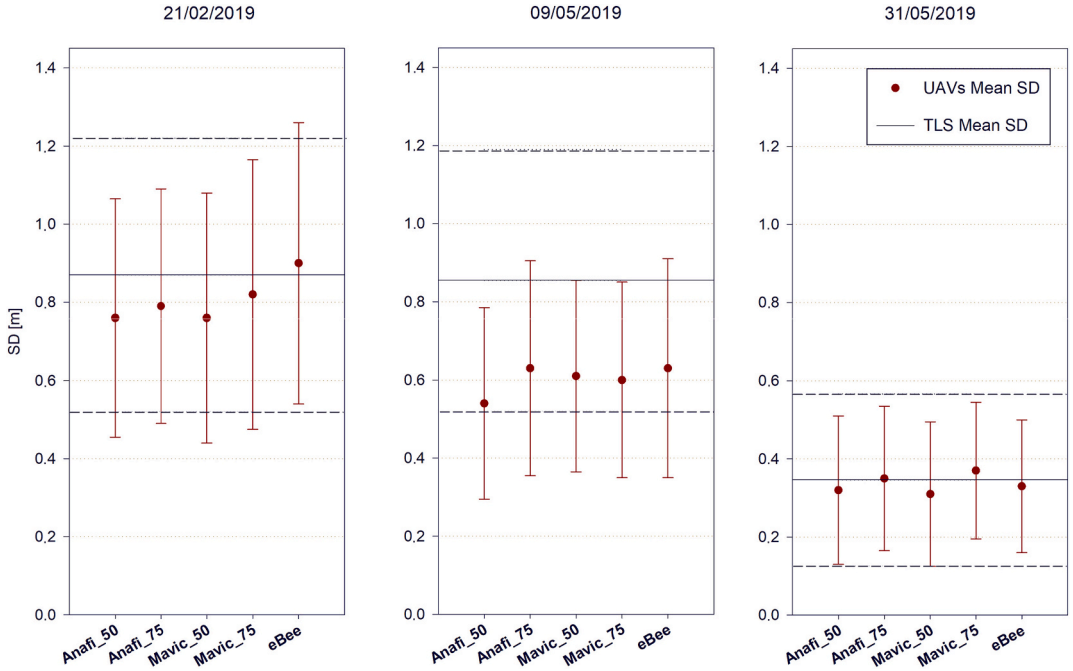

Fig. 7. Mean snow depth (red points) and standard deviations (red lines) obtained from the snow depth maps of the UAVs and with the TLS. Continuous dark lines denote the average snow depth for the reference observation (TLS) and dashed black lines denote the standard deviations of the snow depth for the TLS. (For interpretation of the references to colour in this figure legend, the reader is referred to the web version of this article.)

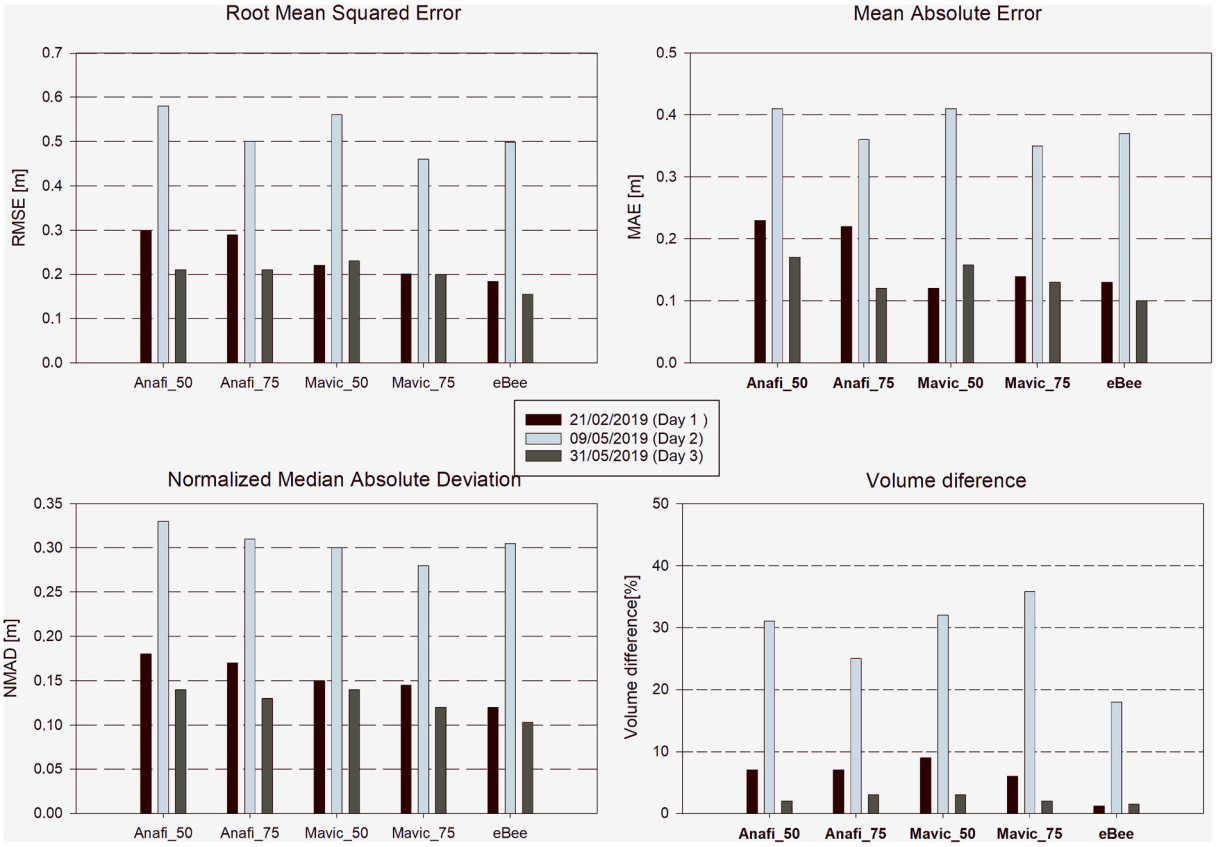

Fig. 8. RMSE (top left panel), MAE (top right panel), NMAD (bottom left panel) volume difference (bottom right panel) obtained in the evaluation of the UAV snow depth maps with the TLS evaluation.

UAV acquisitions is of interest to the snow observations community as recent literature demonstrates (Adams et al., 2018; Avanzi et al., 2018; Bühler et al., 2017; Eberhard et al., 2021; Harder et al., 2016).

Results have clearly shown that under same illumination conditions the three UAV platforms, equipped with cameras of similar characteristics, provide equivalent snow depth products in terms of accuracy. While direct solar radiation lights up the entire study area, the three UAVs provided snow depth maps with an RMSE lower than 0.3 m, MAE of 0.25 m and NMAD below 0.2 m while the total snow volume did not diverge more than 10% from the estimation made with TLS. Despite the slopes of the study area range between 0° and 45°, most of the study site (> 85%) had slopes below 35°. This is important, since deep gullies in the study area are located beneath the steeper areas, and these zones accumulate the higher snow depths (Revuelto et al., 2014b). The occurrence of these high accumulations areas may affect the precision of volume estimations but their reduced extent makes that the impact of the slope in volume difference estimation can be considered as minor.

These error estimates obtained here are in line with previous UAV validation exercises conducted in other study areas (Avanzi et al., 2018; De Michele et al., 2016; Harder et al., 2016). However, under bad illumination conditions the three UAVs failed to properly retrieve the snow surface and thus obtain reliable snow depth observations, with RMSE higher than 0.45 m, MAE above 0.35 m, NMAD over 0.30 m and volume differences higher than 20% for almost all observations. This is because SfM reconstruction is highly impacted by the lack of direct sunlight (Dandois et al., 2015) since, under this condition, the stability and identifiability of image features is highly reduced (Lowe, 2004). Lighting related issues are even more relevant when retrieving snow surfaces since it may have very little contrast (Harder et al., 2016). None of the three platforms compared revealed an advantage to improve snow observation under poor light conditions, a problem that has been identified previously as a major shortcoming when using photogrammetry, with cameras retrieving information in the visible spectrum on snow covered surfaces (Adams et al., 2018). This limitation can be largely reduced when UAVs are equipped with cameras acquiring information in the near infrared bands (Bühler et al., 2017).

Many authors have previously reported either the impossibility of flying with strong winds or significant impact on the quality of UAV snowpack observation under windy conditions (Bühler et al., 2016; Harder et al., 2016). Wind speed constraints encouraged us to plan field campaigns with special attention given to the meteorological forecast and, thus, we avoided acquisitions under unfavourable wind speeds. Illumination and wind restrictions show the major impact that meteorological conditions have in UAV acquisition, regardless of UAV type, since sensors are highly affected by illumination of the target area and the UAV devices have similar wind resistance.

Fixed-wing UAVs are much more efficient and observe larger extents since their flight speed is much higher than that of copter increases flying distance with much lower power, and therefore smaller battery requirements. This allows increased flying distance with a similar battery endurance (De Michele et al., 2016). Fixed-wing devices are definitively recommended when large areas are studied. Conversely, multi-rotors have flight modes and landing systems that deal with complex topography more easily, compared to fixed-wing models (Trujillo et al., 2016). In particular, models with landing procedures similar to that of the *eBee-Plus* may cause problems in rugged terrain, wet surfaces or powder snow. This device lands as an aeroplane, decreasing its flying speed and doing a final gliding with the motor powered down until it impacts to the ground without any 'landing gear'. Fixed-wings devices with vertical take-off and landing (VTOL UAVs, i.e. *wingtra*) may represent a significant improvement in this regard. In addition, although the three models compared are light and easy to transport in a backpack, the two multi-rotors are noticeably smaller and compact, allowing for easier transport as hand luggage for long distance travelling.

Accurately positioning the point cloud generated from the UAV images is required to compare ground/snow surfaces observed on different dates. Usually, artificial targets are placed and used as GCPs within the study area and, once their coordinates have been acquired through indirect methods (differential GPS or total station), GCPs allow an accurate positioning of the point clouds (Fernandes et al., 2018). To date, nearly all UAV works for observing snow distribution have used GCP for precise georeferencing of the point clouds generated with SfM algorithms (Abou Chakra et al., 2020; Adams et al., 2018; Cimoli et al., 2017; Goetz and Brenning, 2019; Harder et al., 2016; Vander Jagt et al., 2013). In contrast, the novel procedure described here to co-registered point clouds to the snow-free model via ICP algorithm has not been widely used. To our knowledge, only two authors have applied before ICP algorithms to georeference dense point clouds in snow covered areas (Abou Chakra et al., 2019; Miziński and Niedzielski, 2017). Vander Jagt et al., (2015) explored other method to co-register the 3D point cloud of a snow-free and a snow-covered UAV acquisition, identifying an unchanging point (snow free) in both observations but always relaying an initial positioning through GCP. Similarly (Nolan et al., 2015) tested an equivalent co-registration using the full extent of their observations as pseudo GCPs, but in this case with an initial accurate positioning system available in manned aircrafts. Placing GCPs in rugged mountain areas is an important drawback of UAVs, since some locations of complex study areas may be unreachable or endanger technical staff. The good results obtained in this research and previous works (Abou Chakra et al., 2019; Miziński and Niedzielski, 2017) to accurately geolocate dense point cloud with ICP algorithms may avoid the use of GCPs to retrieve the snow distributions with UAVs in many study areas.

Currently UAVs are not able to acquire information for very large areas (as far authors know the largest UAV snow observation reaches 4 km^2 (Eberhard et al., 2021)), when increasing the surveyed areas, the geolocation of UAV images may face ellipsoid and geoid derived problems and thus the selection of the coordinate system (projected or not) will be extremely relevant.

In view of GCP drawbacks, for two out of the three acquisition dates, we tested an alternative georeferencing method for devices without RTK.. Through an ICP alignment of the snow-free areas to the snow-free point cloud, we were able to obtain an accurate registration of the point cloud. In turn, this allowed generation of reliable snow depth distribution maps, as the evaluation metrics revealed while direct sunlight illuminated the study area. The major disadvantage of this registration method is the necessity of snow-free areas occurring within the study area to enable ICP alignment to the snow-free point cloud. Once the test site is not fully snow covered (results show at least a 25% snow-free area is needed; see SCA temporal evolution in Fig. 2) and taking advantage of the repeated snow-free area patterns observed during the melting period (Revuelto et al., 2020; Sturm and Wagner, 2010), this co-registration method may allow observation of the snow surface with low-cost UAVs (which do now allow RTK positioning accuracies) and without GCP being placed within the study area. Nonetheless, the minimum snow-free area extent to obtain a reliable ICP co-registration may depend on the spatial distribution of the snow covered area. The snow distribution for the 9 and 31 May 2019 was heterogeneous and at the same time, the snow-free areas occurred in diverse locations, covering several sectors of the scene. Probably if the snow-free areas are found in the same area of the test site the performance of this procedure would decrease.

Another georeferencing method, in absence of snow-free areas and GCPs, accurate enough to observe snow distribution in remote mountain areas, are UAVs having RTK processing of the GPS signal (or the alternative PPK Post-Processed Kinematic of GPS signal). This way, in the last two years some authors have evaluated the reliability of snow depth observations with UAVs having GPS with RTK positioning (Eberhard et al., 2021; Gabrlik et al., 2019; Harder et al., 2020). Despite these later studies only used some sparse snow observations to evaluate UAV acquisitions, they shown compelling results when observing the snowpack. Similarly, the TLS evaluation of UAV with RTK positioning presented

here (the fixed-wing device), has revealed reliable snow depth observations under good illumination conditions. The similar results obtained when observing the snowpack with UAVs, regardless the georeferencing method (GCPs, ICP of RTK) is a highly valuable outcome of this study. This demonstrates that GCP positioning can be replaced by alternative methods without decreasing the accuracy of the observation, largely reducing exposure to mountain risks and also enabling a simpler post-processing of the information, compared to acquisitions requiring GCPs.

The UAV flight altitude tested here has revealed a minor impact on the quality of snow depth maps. In contrast other authors found image height above ground as one of the variables with greatest explanatory power on the precision of Digital Elevations Models derived from UAV observations (Goetz et al., 2018). Other authors also highlighted the importance of choosing suitable flight altitudes for required resolutions, suggesting that flight altitudes of 100 m us sufficient for the survey of snow cover (Abou Chakra et al., 2020). Probably, the high resolution of sensors that are mounted on commercial UAVs and the dissimilar evaluation accomplished here (evaluation of snow depth observations), may be behind the negligible impact of the mean sensor-target distance (we changed from 50 m to 75 m) obtained on the quality of the final product. However better evaluation scores were obtained for the 75 m flight altitude with the two multi-rotors. This result is probably related to a better lateral overlap of the photos when flying at higher altitudes, which is more beneficial than the enhanced resolution obtained when flying closer to the surface. Furthermore higher altitudes are also associated with larger pixels sizes that are associated with improved SfM solution but less dense point clouds (Dandois et al., 2015). Higher elevations additionally guarantee safer acquisitions and reduce the time of flights, likely obtaining more reliable snowpack observations.

This study shows that when selecting a UAV platform, the price of the product is not a major constraint for obtaining good quality results when observing the cryosphere, if a well-established acquisition and post-processing protocol is established (Gaffey and Bhardwaj, 2020). Indeed, the three models compared here have proved to have good stability and proper acquisition of images within, when the wind operation thresholds are respected. Nonetheless for a safe UAV flight low wind speeds are recommended. Even if the accuracy of snow maps could be slightly lower than with TLS, UAVs have shown clear advantages regarding the former technique, as UAV acquisition are affected very little by topographic shadows, allowing acquisition of information for almost the entire study area. In addition, UAVs are definitively lighter than TLS devices (a weight ratio higher than 10), enabling much easier displacement in mountain areas. TLS presents obvious advantages when working on shallow snowpacks and where greater accuracy is required, or when there is not clear sky conditions. TLS performance is not affected by solar illumination issues such as cloud presence (Prokop, 2008) or low solar elevation angles (likely during winter period) causing large cast shadows from surrounding topography. According to the study results, the selection of UAV to perform snow mapping should be mostly based on three main considerations - the size of the study area to observe, the topographic complexity of the area to be mapped, and the possibility/ease of placing GCPs.

6. Conclusions

Despite the increased number of works using UAVs to observe snowpack evolution in mountain areas, none of them has compared concurrent acquisitions of commercial devices. This motivated us to generate snow depth maps in a small but highly heterogeneous test area, following the same post-processing protocol with images obtained from three different UAV platforms. This consisted of two multi-rotors devices without RTK-GPS and a fixed-wing UAV with RTK-GPS positioning, equipped with cameras of similar characteristics. Results were tested against TLS acquisition, which is considered the most accurate technique to generate high spatial resolution snow depth maps. Despite the noticeable differences among the three UAVs tested, the quality of the snow maps was very similar, and it was almost impossible to discern which was the most/least precise. Under good illumination conditions, and flying around midday to guarantee a homogenous illumination of the domain, the three UAVs provided high quality snow depth maps with an average RMSE lower than 0.22 m, compared to the TLS acquisition. When clouds impeded direct solar illumination, the quality dramatically decreased in the products derived with images of the three platforms, with errors (RMSE larger than 0.45 m and NMAD above 0.3 m) that prevented proper estimation of the total volume of snow (deviations higher than 20% when compared to TLS observations). Acquisitions obtained under good illumination conditions represented an advantage over those acquired with TLS, as the bird's-eye point of view permitted retrieval of information for nearly the whole study area, compared to 77% of the area covered with TLS. Flight altitudes tested here revealed a minor impact on observations of snow distribution. Nonetheless, slightly worse scores were obtained with the lower elevation flying paths. Thus, flying at higher elevations is not only safer and more efficient in terms of flight duration, but is also more recommended in order to obtain more accurate snow depth maps. The similar results obtained with the three UAV platforms suggest that the following should be taken into account when acquiring a new UAV device: whether or not extended areas will be covered, as fixed-wing devices have landing constraints (vertical versus a final UAV gliding); the possibility of georeferencing the information through GCP; and applying an ICP alignment on unaltered surfaces during the study period or the need of having RTK positioning.

Authors statement

All authors have seen and approved the final version of the manuscript being submitted.

Declaration of Competing Interest

The authors declare that they have no known competing financial interests or personal relationships that could have appeared to influence the work reported in this paper.

Acknowledgments

This work was supported by the research projects of the Spanish Ministry of Economy and Competitiveness projects “El papel de la nieve en la hidrología de la península ibérica y su respuesta a procesos de cambio global- CGL2017-82216-R” and the JPI-Climate co-funded call of the European Commission and INDECIS and CROSSDRO which are part of ERA4CS, and ERA-NET. Authors do not have any conflict of interest.). J. Revuelto is supported by a “Juan de la Cierva Incorporación” postdoctoral fellow of the Spanish Ministry of Science, Innovation and Universities (Grant IJC2018-036260-I). I. Vidaller is supported by the Grant FPU18/04978 and is studying in the PhD program in the University of Zaragoza (Earth Science Department).

Appendix A. Supplementary data

Supplementary data to this article can be found online at https://doi.org/10.1016/j.coldregions.2021.103344.

References

Abou Chakra, C., Gascoin, S., Somma, J., Fanise, P., Drapeau, L., 2019. Monitoring the snowpack volume in a Sinkhole on Mount Lebanon using time lapse photogrammetry. Sensors 19, 3890.

Abou Chakra, C., Somma, J., Gascoin, S., Fanise, P., Drapeau, L., 2020. Impact of flight altitude on unmanned aerial photogrammetric survey of the snow height on mount lebanon. ISPRS - International Archives of the Photogrammetry. Remote Sens. Spatial Inform. Sci. 43B2, 119–125.

Adams, M.S., Bühler, Y., Fromm, R., 2018. Multitemporal accuracy and precision assessment of unmanned aerial system photogrammetry for slope-scale snow depth maps in alpine terrain. Pure Appl. Geophys. 175, 3303.
Agüera-Vega, F., Carvajal-Ramírez, F., Martínez-Carricondo, P., 2017. Accuracy of digital surface models and orthophotos derived from unmanned aerial vehicle photogrammetry. J. Surv. Eng. 143, 04016025.
Anderton, S.P., White, S.M., Alvera, B., 2002. Micro-scale spatial variability and the timing of snow melt runoff in a high mountain catchment. J. Hydrol. 268, 158–176.
Anderton, S.P., White, S.M., Alvera, B., 2004. Evaluation of spatial variability in snow water equivalent for a high mountain catchment. Hydrol. Process. 18, 435–453.
Avanzi, F., Bianchi, A., Cina, A., De Michele, C., Maschio, P., Pagliari, D., Passoni, D., Pinto, L., Piras, M., Rossi, L., 2018. Centimetric accuracy in snow depth using unmanned aerial system photogrammetry and a multistation. Remote Sens. 10, 765.
Besl, P.J., McKay, N.D., 1992. Method for registration of 3-D shapes. In: Sensor Fusion IV: Control Paradigms and Data Structures. International Society for Optics and Photonics, pp. 586–606.
Boesch, R., Bühler, Y., Marty, M., Ginzler, C., 2016. Comparison of digital surface models for snow depth mapping with UAV and aerial cameras. Int. Arch. Photogramm. Remote. Sens. Spat. Inf. Sci. *XLI-B8*, 453–458.
Bühler, Y., Adams, M.S., Bösch, R., Stoffel, A., 2016. Mapping snow depth in alpine terrain with unmanned aerial systems (UASs): potential and limitations. Cryosphere 10, 1075.
Bühler, Y., Adams, M.S., Stoffel, A., Boesch, R., 2017. Photogrammetric reconstruction of homogenous snow surfaces in alpine terrain applying near-infrared UAS imagery. Int. J. Remote Sens. 38, 3135–3158.
Chang, T., Yu, H., 2015. Improving electric powered UAVs' endurance by incorporating battery dumping concept. Proc. Eng. 99, 168–179.
Cimoli, E., Marcer, M., Vandecrux, B., Bøggild, C.E., Williams, G., Simonsen, S.B., 2017. Application of low-cost UASs and digital photogrammetry for high-resolution snow depth mapping in the arctic. Remote Sens. 9, 1144.
Corripio, J.G., 2004. Snow surface albedo estimation using terrestrial photography. Int. J. Remote Sens. 25, 5705–5729.
Dandois, J.P., Olano, M., Ellis, E.C., 2015. Optimal altitude, overlap, and weather conditions for computer vision UAV estimates of forest structure. Remote Sens. 7, 13895–13920.
De Michele, C.D., Avanzi, F., Passoni, D., Barzaghi, R., Pinto, L., Dosso, P., Ghezzi, A., Gianatti, R., Vedova, G.D., 2016. Using a fixed-wing UAS to map snow depth distribution: an evaluation at peak accumulation. Cryosphere 10, 511–522.
Deems, J.S., Painter, T.H., Finnegan, D.C., 2013. Lidar measurement of snow depth: a review. J. Glaciol. 59, 467–479.
Eberhard, L.A., Sirguey, P., Miller, A., Marty, M., Schindler, K., Stoffel, A., Bühler, Y., 2021. Intercomparison of photogrammetric platforms for spatially continuous snow depth mapping. Cryosphere 15, 69–94.
Fayad, A., Gascoin, S., Faour, G., López-Moreno, J.I., Drapeau, L., Le Page, Michel, Escadafal, R., 2017. Snow hydrology in Mediterranean mountain regions: a review. J. Hydrol. 551, 374–396.
Fernandes, R., Prevost, C., Canisius, F., Leblanc, S.G., Maloley, M., Oakes, S., Holman, K., Knudby, A., 2018. Monitoring snow depth change across a range of landscapes with ephemeral snowpacks using structure from motion applied to lightweight unmanned aerial vehicle videos. The Cryosphere; Katlenburg-Lindau 12, 3535–3550.
Forlani, G., Dall'Asta, E., Diotri, F., di Cella, U.M., Roncella, R., Santise, M., 2018. Quality assessment of DSMs produced from UAV flights georeferenced with on-board RTK positioning. Remote Sens. 10, 311.
Frei, A., Tedesco, M., Lee, S., Foster, J., Hall, D.K., Kelly, R., Robinson, D.A., 2012. A review of global satellite-derived snow products. Adv. Space Res. 50, 1007–1029.
Gabrlik, P., Janata, P., Zalud, L., Harcarik, J., 2019. Towards automatic UAS-based snow-field monitoring for microclimate research. Sensors 19, 1945.
Gaffey, C., Bhardwaj, A., 2020. Applications of unmanned aerial vehicles in cryosphere: latest advances and prospects. Remote Sens. 12, 948.
Gindraux, S., Boesch, R., Farinotti, D., 2017. Accuracy assessment of digital surface models from unmanned aerial vehicles' imagery on glaciers. Remote Sens. 9, 186.
Goetz, J., Brenning, A., 2019. Quantifying uncertainties in snow depth mapping from structure from motion photogrammetry in an alpine area. Water Resour. Res. 55 https://doi.org/10.1029/2019WR025251.
Goetz, J., Brenning, A., Marcer, M., Bodin, X., 2018. Modeling the precision of structure-from-motion multi-view stereo digital elevation models from repeated close-range aerial surveys. Remote Sens. Environ. 210, 208–216.
Grünewald, T., Lehning, M., 2015. Are flat-field snow depth measurements representative? A comparison of selected index sites with areal snow depth measurements at the small catchment scale. Hydrol. Process. 29, 1717–1728.
Grünewald, T., Schirmer, M., Mott, R., Lehning, M., 2010. Spatial and temporal variability of snow depth and ablation rates in a small mountain catchment. Cryosphere 4, 215–225.
Harder, P., Schirmer, M., Pomeroy, J., Helgason, W., 2016. Accuracy of snow depth estimation in mountain and prairie environments by an unmanned aerial vehicle. Cryosphere 10, 2559–2571.
Harder, P., Pomeroy, J.W., Helgason, W.D., 2020. Improving sub-canopy snow depth mapping with unmanned aerial vehicles: lidar versus structure-from-motion techniques. Cryosphere 14, 1919–1935.
Hock, R., 2005. Glacier melt: a review of processes and their modelling. Prog. Phys. Geogr. 29, 362–391.
Hock, R., Hutchings, J.K., Lehning, M., 2017. Grand challenges in cryospheric sciences: toward better predictability of glaciers, snow and sea ice. Front. Earth Sci. 5.
Höhle, J., Höhle, M., 2009. Accuracy assessment of digital elevation models by means of robust statistical methods. ISPRS J. Photogramm. Remote Sens. 64, 398–406.
James, M.R., Robson, S., Smith, M.W., 2017. 3-D uncertainty-based topographic change detection with structure-from-motion photogrammetry: precision maps for ground control and directly georeferenced surveys. Earth Surf. Process. Landf. 42, 1769–1788.
Lague, D., Brodu, N., Leroux, J., 2013. Accurate 3D comparison of complex topography with terrestrial laser scanner: Application to the Rangitikei canyon (N-Z). ISPRS J. Photogramm. Remote Sens. 82, 10–26.
López-Moreno, J., 2005. Recent variations of snowpack depth in the central Spanish pyrenees. Arct. Antarct. Alp. Res. 37, 253–260.
López-Moreno, J.I., Latron, J., Lehmann, A., 2010. Effects of sample and grid size on the accuracy and stability of regression-based snow interpolation methods. Hydrol. Process. 24, 1914–1928.
López-Moreno, J.I., Fassnacht, S.R., Beguería, S., Latron, J.B.P., 2011. Variability of snow depth at the plot scale: implications for mean depth estimation and sampling strategies. Cryosphere 5, 617–629.
López-Moreno, J.I., Pomeroy, J.W., Revuelto, J., Vicente-Serrano, S.M., 2012. Response of snow processes to climate change: spatial variability in a small basin in the Spanish Pyrenees. Hydrol. Process. 27, 2637–2650.
López-Moreno, J.I., Revuelto, J., Fassnacht, S.R., Azorín-Molina, C., Vicente-Serrano, S. M., Morán-Tejeda, E., Sexstone, G.A., 2015. Snowpack variability across various spatio-temporal resolutions. Hydrol. Process. 29, 1213–1224.
Lowe, D.G., 2004. Distinctive image features from scale-invariant keypoints. Int. J. Comput. Vis. 60, 91–110.
Miziński, B., Niedzielski, T., 2017. Fully-automated estimation of snow depth in near real time with the use of unmanned aerial vehicles without utilizing ground control points. Cold Reg. Sci. Technol. 138, 63–72.
Nolan, M., Larsen, C., Sturm, M., 2015. Mapping snow depth from manned aircraft on landscape scales at centimeter resolution using structure-from-motion photogrammetry. Cryosphere 9, 1445.
Parajka, J., Blöschl, G., 2008. Spatio-temporal combination of MODIS images – potential for snow cover mapping. Water Resour. Res. *44* n/a-n/a.
Parajka, J., Haas, P., Kirnbauer, R., Jansa, J., Blöschl, G., 2012. Potential of time-lapse photography of snow for hydrological purposes at the small catchment scale. Hydrol. Process. 26, 3327–3337.
Pomeroy, J., Essery, R., Toth, B., 2004. Implications of spatial distributions of snow mass and melt rate for snow-cover depletion: observations in a subarctic mountain catchment. Ann. Glaciol. 38, 195–201.
Prokop, A., 2008. Assessing the applicability of terrestrial laser scanning for spatial snow depth measurements. Cold Reg. Sci. Technol. 54, 155–163.
Rajendra, Y.D., Mehrotra, S.C., Kale, K.V., Manza, R.R., Dhumal, R.K., Nagne, A.D., Vibhute, A.D., 2014. Evaluation of Partially Overlapping 3D Point Cloud's Registration by using ICP variant and CloudCompare. In: The International Archives of Photogrammetry, Remote Sensing and Spatial Information Sciences, pp. 891–897. Gottingen, (Gottingen, Germany, Gottingen: Copernicus GmbH).
Réveillet, M., Vincent, C., Six, D., Rabatel, A., 2017. Which empirical model is best suited to simulate glacier mass balances? J. Glaciol. 63, 39–54.
Revuelto, J., López-Moreno, J.I., Azorin-Molina, C., Zabalza, J., Arguedas, G., Vicente-Serrano, S.M., 2014a. Mapping the annual evolution of snow depth in a small catchment in the Pyrenees using the long-range terrestrial laser scanning. J. Maps 10, 1–15.
Revuelto, J., López-Moreno, J.I., Azorin-Molina, C., Vicente-Serrano, S.M., 2014b. Topographic control of snowpack distribution in a small catchment in the central Spanish Pyrenees: Intra- and inter-annual persistence. Cryosphere 8, 1989–2006.
Revuelto, J., Jonas, T., López-Moreno, J.-I., 2016a. Backward snow depth reconstruction at high spatial resolution based on time-lapse photography. Hydrol. Process. 30, 2976–2990.
Revuelto, J., Vionnet, V., López-Moreno, J.I., Lafaysse, M., Morin, S., 2016b. Combining snowpack modeling and terrestrial laser scanner observations improves the simulation of small scale snow dynamics. J. Hydrol. 291–307.
Revuelto, J., Azorin-Molina, C., Alonso-González, E., Sanmiguel-Vallelado, A., Navarro-Serrano, F., Rico, I., López-Moreno, J.I., 2017. Meteorological and snow distribution data in the Izas Experimental Catchment (Spanish Pyrenees) from 2011 to 2017. Earth Syst. Sci. Data 9, 993–1005.
Revuelto, J., González, E.A., López-Moreno, J.I., 2020. Generation of daily high-spatial resolution snow depth maps from in-situ measurement and time-lapse photographs. Cuadernos Invest. Geogr. 46 (1), 59–79.
Revuelto, J., González, E.A., López- Moreno, J.I., 2021. Light and shadow in mapping alpine snowpack with unmanned aerial vehicles in the absence of ground control points. Water Res. Res. 57, e2020WR028980 https://doi.org/10.1029/2020WR028980.
Schön, P., Naaim-Bouvet, F., Vionnet, V., Prokop, A., 2018. Merging a terrain-based parameter with blowing snow fluxes for assessing snow redistribution in alpine terrain. Cold Reg. Sci. Technol. 155, 161–173.
Snavely, N., Seitz, S.M., Szeliski, R., 2006. Photo Tourism: Exploring Photo Collections in 3D, pp. 835–846.
Sturm, M., Wagner, A.M., 2010. Using repeated patterns in snow distribution modeling: An Arctic example. Water Resour. Res. 46.
Traub, L.W., 2011. Range and Endurance estimates for Battery-Powered Aircraft. J. Aircr. 48, 703–707.
Trujillo, M.M., Darrah, M., Speransky, K., DeRoos, B., Wathen, M., 2016. Optimized flight path for 3D mapping of an area with structures using a multirotor. In: In 2016 International Conference on Unmanned Aircraft Systems (ICUAS), pp. 905–910.

Vander Jagt, B.J., Durand, M.T., Margulis, S.A., Kim, E.J., Molotch, N.P., 2013. The effect of spatial variability on the sensitivity of passive microwave measurements to snow water equivalent. Remote Sens. Environ. 136, 163–179.
Vander Jagt, B., Lucieer, A., Wallace, L., Turner, Darren, Durand, M., 2015. Snow Depth Retrieval with UAS using Photogrammetric Techniques. Geosciences 5, 264–285.
Westoby, M.J., Brasington, J., Glasser, N.F., Hambrey, M.J., Reynolds, J.M., 2012. 'Structure-from-Motion' photogrammetry: a low-cost, effective tool for geoscience applications. Geomorphology 179, 300–314.